Published in final edited form as:

Gastro Hep Adv. 2023 ; 2(4): 532–543. doi:10.1016/j.gastha.2023.02.003.

Transcriptional Profile of Human Pancreatic Acinar Ductal Metaplasia

Jinmai Jiang[1,*], **Hesamedin Hakimjavadi**[2,3,*], **Julie K. Bray**[2], **Corey Perkins**[1,3], **Alyssa Gosling**[1], **Lais daSilva**[1], **Gamze Bulut**[1], **Jamel Ali**[4,3], **V. Wendy Setiawan**[5,3], **Martha Campbell-Thompson**[2,3], **Srikar Chamala**[2,3], **Thomas D. Schmittgen**[1,3]

[1]Department of Pharmaceutics, College of Pharmacy University of Florida, Gainesville, Florida

[2]Department of Pathology, Immunology, and Laboratory Medicine, College of Medicine, University of Florida, Gainesville, Florida

[3]Florida-California Cancer Research, Education and Engagement (CaRE[2]), Health Equity Center, Gainesville, Florida

[4]Department of Chemical and Biomedical Engineering, FAMU-FSU College of Engineering, Tallahassee, Florida

[5]Department of Epidemiology, Keck School of Medicine, University of Southern California, Los Angeles, California

Abstract

BACKGROUND AND AIMS: Aberrant acinar to ductal metaplasia (ADM), one of the earliest events involved in exocrine pancreatic cancer development, is typically studied using pancreata from genetically engineered mouse models.

Correspondence: Address correspondence to: Thomas D. Schmittgen, PhD, P.O. Box 103633, Gainesville, Florida 32610. tschmittgen@ufl.edu. Srikar Chamala, PhD, 4640 West Sunset Blvd, Los Angeles, California 90027. schamala@chla.usc.edu.
*These authors contributed equally to this work.

Authors' Contributions:
Jinmai Jiang: Study design, performed experiments, data analysis, and interpretation of data. Hesamedin Hakimjavadi: Study design, data analysis, writing (primary), and editing (primary) of the manuscript. Julie K. Bray: Performed experiments. Alyssa Gosling: Performed experiments. Lais daSilva: Performed experiments. Gamze Bulut: Performed experiments. Corey Perkins: Performed experiments. Jamel Ali: Discussions and interpretation of data. V. Wendy Setiawan: Discussions and interpretation of data. Martha Campbell-Thompson: Discussions, editing the manuscript, and interpretation of data. Srikar Chamala: Data analysis and editing of the manuscript. Thomas D. Schmittgen: Study design, interpretation of data, writing (primary), and editing (primary) of the manuscript.

Conflicts of Interest:
The authors disclose no conflicts.

Ethical Statement:
The corresponding author, on behalf of all authors, jointly and severally, certifies that their institution has approved the protocol for any investigation involving humans or animals and that all experimentation was conducted in conformity with ethical and humane principles of research.

Data Transparency Statement:
All curated datasets were posted to the Gene Expression Omnibus (GEO) repository under accession number GSE179248.

Reporting Guidelines:
Helsinki Declaration, STROBE, SAGER.

Supplementary materials
Material associated with this article can be found in the online version at https://doi.org/10.1016/j.gastha.2023.02.003.

METHODS: We used primary, human pancreatic acinar cells from organ donors to evaluate the transcriptional and pathway profiles during the course of ADM.

RESULTS: Following 6 days of three-dimensional culture on Matrigel, acinar cells underwent morphological and molecular changes indicative of ADM. mRNA from 14 donors' paired cells (day 0, acinar phenotype and day 6, ductal phenotype) was subjected to whole transcriptome sequencing. Acinar cell specific genes were significantly downregulated in the samples from the day 6 cultures while ductal cell–specific genes were upregulated. Several regulons of ADM were identified including transcription factors with reduced activity (PTF1A, RBPJL, and BHLHA15) and those ductal and progenitor transcription factors with increased activity (HNF1B, SOX11, and SOX4). Cells with the ductal phenotype contained higher expression of genes increased in pancreatic cancer while cells with an acinar phenotype had lower expression of cancer-associated genes.

CONCLUSION: Our findings support the relevancy of human in vitro models to study pancreas cancer pathogenesis and exocrine cell plasticity.

Keywords

Acinar ductal metaplasia; Pancreas; Pancreatic cancer; Organoid

Introduction

Pancreatic ductal adenocarcinoma (PDAC) is among the most lethal of all cancers with a 5-year survival of only 10%.[1] PDAC is predicted to become the second most deadly cancer in the United States by 2030.[2] Invasive PDAC develops via low-grade to high-grade precursor lesions known as pancreatic intraepithelial neoplasia (PanIN).[3] PanIN-2 is typically proceeded by activating mutations in *KRAS*, an oncogene that is mutated in more than 90% of PDAC. Studying the early events in the development of human PDAC is challenging because the disease is often diagnosed in patients at a late stage, often once the tumor has metastasized. For these reasons, PDAC pathogenesis is more often studied in genetically modified mouse models (GEMMs).[4–7]

Studies in GEMMs reveal an underlying role for pancreatic acinar cells in PDAC development.[8–11] In mice, PanINs are preceded by the process of acinar ductal metaplasia (ADM).[12,13] The hallmarks of ADM include loss of zymogen granules, the transdifferentiation of acini into duct-like structures with reduced expression of acinar markers such as amylase (AMY2A) or carboxypeptidase (CPA2), and increased ductal markers such as cytokeratin 19 (KRT19). ADM is a natural process that occurs following pancreatic injury to protect acinar cells from further damage. In mouse models of PDAC, ADM is achieved by restricted expression of Kras in acinar cells,[11,14] pancreatitis,[15] TGF-α,[16] or other factors that activate EGFR.[13] ADM is believed to be irreversible in GEMMs with mutant *Kras*, under conditions of aberrant growth factor signaling or in situations with altered expression of key drivers of the process.[17–19] We recently reported that pancreatic ductal cells that have underwent ADM can be pharmacologically reversed in vitro to a more acinar phenotype.[20] Using an inducible form of mutant *Kras*, Collins et al. showed that PanINs revert to ADMs and eventually to acinar cells following *Kras* inactivation

upon doxycycline withdraw.[4] In the context of mutant *KRAS*, dedifferentiated acinar cells are believed to give rise to PDAC that is akin to the classical subtype while ductal cells presumably give rise to a basal-like subtype that is characterized with worse survival outcome.[21]

ADM is commonly studied in vitro using three-dimensional (3-D) cultures by plating mouse acini on the extracellular matrix Matrigel or on collagen supplemented with TGF-α.[4,13,22,23] While a role for ADM in the development of PDAC in mice has been established, evidence for the contributions of ADM in the development of human PDAC is still unknown. ADM has been less well studied in humans due to a scarcity of human acinar cells for research. Limitations of human acinar tissues for biomedical research are due in part to the secluded anatomic location of the pancreas precluding safe biopsy and a lack of nontransformed human acinar cell lines. ADM culture has been performed with human pancreatic acini using nonislet cell fractions of normal primary human pancreatic exocrine cell acini obtained from islet isolation centers.[24–27] Whole transcriptome RNA sequencing of FACS sorted acinar and ductal cells identified that the transcriptional regulator MECOM was unique for dedifferentiated acinar cells and that MECOM suppresses acinar cell death by permitting cellular dedifferentiation.[24] Reported here are key modifications to existing protocols that allowed for successful 3-D culture and transdifferentiation of human pancreatic acini. Our findings demonstrate that regulation of many of the transcription factors and pathways that occur in PDAC are recapitulated using this human organoid model of normal pancreatic acini.

Results

Primary human acinar cultures for studying pancreatic ADM

Fresh islet-depleted pancreas digests were shipped in culture media on ice packs and received within 24 h from collaborating islet isolation centers. Cells were suspended in Matrigel and their ability to undergo ADM was monitored daily. The Matrigel media collapsed during the 6-day incubation from 4 of the first 8 donors' cultures. To address this concern, soybean trypsin inhibitor was added to inactive any trypsin that may be released and compromising the Matrigel integrity (Figure A1A and B). Liu et al.[27] cultured primary human acinar cells in serum-free conditions in Matrigel plus TGF-β. These conditions were attempted here; however, adding 0.5 ng/mL of TGF-β to the culture media did not enhance ADM but inhibited it and therefore all cultures were performed without TGF-β supplement (Figure A1C). Once these modifications were made, we maintained viability and successfully performed transdifferentiation to ductular morphology on 36 of 36 organoid cultures. Shown in Figure 1A are the cell viability and transdifferentiation from 10 of the acinar cultures. To isolate RNA with high integrity for gene expression analysis, cells were separated from the Matrigel using a protocol recently published by our group.[28] Using these modifications, RNA with RINs of 7 or more was isolated from 14 pairs of samples (Table A1). qRT-PCR was performed on the day 0 and day 6 RNA and demonstrated reduction of acinar and increase in ductal and progenitor gene expression (Figure 1B).

Twenty five percent of protein coding genes are differentially expression during ADM

Total RNA from 14 pairs of day 0 and day 6 cells was sequenced using Novoseq 6000, generating an average of 86,000 reads per sample. Unsupervised hierarchical clustering was performed on the 14 pairs of samples to determine the association between transcriptional profiles, ADM status, and demographic data collected from each donor. Unsupervised hierarchical clustering of the top 2000 most differentially expressed genes indicates that the transcriptional response profiles for cells undergoing 6 days of ADM clustered tightly and were completely distinguished from the baseline cells collected at day 0 (Figure 2A). Principal component analysis (PCA) of all expressed protein coding genes shows 4 distinct clusters that are matched to the ADM status of samples and donor's gender (Figure 2B).

Applying K-Means unsupervised clustering on the top 2000 most differentially expressed genes, we identified 3 distinct clusters based on their expression pattern across all samples (Figure A2A). Of these 3 clusters, 2 consist of genes mostly upregulated (cluster A) or downregulated (cluster B) in the day 6 ADM samples (cluster A: ductal cluster, cluster B: acinar cluster). Enrichment analysis revealed that pathways enriched in the cluster B are those involved in pancreatic secretion, protein digestion and absorption, starch and sucrose metabolism, and MAPK signaling pathway, thus validating the association of this cluster to the acinar phenotype (Figure A2B). Noticeably 2 cancer-related KEGG pathways, chemical carcinogenesis and proteoglycans in cancer, are enriched in the ductal cluster ($P < .0001$ and $P = .0011$, respectively). To obtain statistically significant genes, enriched pathways and transcription factors, we compared the transcription level of protein coding genes between human primary cells at day 6 vs day 0 of ADM.

A total of 4575 transcripts were identified as differentially expressed between day 6 vs day 0 of ADM (fold change more than or less than 2, $P < .05$). Of these differentially expressed genes, 2509 genes (12.9% of total protein coding genes) were upregulated and 2066 genes (10.6% of total) were downregulated in day 6 vs day 0 of ADM (Figure 2C). As anticipated, the expression of a number of acinar genes and transcription factors were reduced at day 6 of ADM including CEL, CELA1, PNLIP, PRSS2, BHLHA15, PTF1A, and RBPJL (Figure 3). Many ductal-associated and progenitor (eg, CFTR, KRT17, HNF1B, PROM1, and EPCAM) and cancer-associated (TGFB1, EGFR, MMP14, IGF1R, and ITGB1) genes were increased at day 6 of ADM. In general, collagens were increased at day 6 (eg, COLO10A1, COL11A1, and COL1A1; Figure 3).

Identification of ADM regulators

Gene Set Enrichment Analysis (GSEA) was applied to the RNA sequencing data obtained at day 0 and day 6. Performing GSEA on 6449 curated gene sets, including a number of canonical pathways such as KEGG and Biocarta, yielded those gene sets that are negatively enriched in acinar cells at day 0 and those gene sets that are positively enriched in ductal cells at day 6. Interestingly, the top ductal enriched gene sets were those genes upregulated in pancreatic cancer (Figure 4A). All of the top enriched gene sets in the day 6 ductal cells are multicancer invasive signature, those associated with collagen fibrils and collagen degradation and TGFβ-regulated epithelial mesenchymal transition. The top 5 pathways negatively enriched in the day 6 acinar cells are those related to translation (Figure 4A).

GSEA was used to identify the top transcription factors that regulate ADM. We identified 40 regulons positively or negatively correlated with upregulated and downregulated genes at day 6 of ADM using a two-tailed GSEA. SOX11 and RBPJL are examples of transcription factors with positive (ADM driver) and negative (acinar driver) enrichment scores, respectively (Figure 4B and C). The acinar driver regulons include GATA4, PTF1A, RBPJL, and BHLHA15 whose activity is reduced at day 6 of ADM (Figure 4D). ADM driver genes, those genes with increased activity at day 6, include HNF1B, SOX4, SOX11, STAT2, and STAT6.

Ingenuity pathway analysis was used to identify the top upstream pathways regulating ADM. The top activated upstream growth factor regulated pathways during human ADM include TGFB1, TGFB2, and TGFB3 (Table 1) while the top upstream cytokine-regulated pathways activated during ADM include several interleukins and interferons (Table 2). We then compared the top 10 upstream regulators from our in vitro human ADM to those literature data[12] obtained from laser microdissected mouse tissues undergoing ADM in vivo. Interestingly, there was a fair degree of overlap between the 2 datasets including the top 2 ranked pathways angiotensinogen (AGT) and TGFB1 (Table 1). TNF was the top activated cytokine in both the human and mouse datasets; other overlapping cytokines include IL1A and oncostatin M (OSM) (Table 2).

Co-regulation and inference of dual regulons

Following RTNduals workflow,[29] we re-analyzed pairs of regulons identified in the previous section to classify sets of ADM-associated transcriptional regulators with shared targets/regulons (dual regulons). We identified 103 transcription factors that form 335 dual regulons with a significant overlap. Among the significant dual regulons are RBPJL ~ SOX4 and BHLHA15~RBPJL. RBPJL ~ SOX4 is an example of a dual regulon in which the regulators cooperate by influencing the shared target genes in the opposite direction (Figure A3) while BHLHA15~RBPJL is a dual regulon that influences shared target genes in the same direction (Figure A4). For the RBPJL ~ SOX4 dual regulon, RBPJL has a negative enrichment score while SOX4 is positive (Figure A3A and B). Four of the many overlapping genes of the BHLHA15~SOX4 dual regulon were selected for further analysis including the acinar genes CPA1 and AMY2A and the tumor associated genes ITGB1 and MMP14. Comparing the day 0 and day 6 gene expression of RBPJL to the acinar and tumor genes showed indirect correlations between RBPJL and the tumor genes (Figure A3C and E) and a direct correlation between RBPJL with AMY2A or CPA1 (Figure A3G and I). Correlations in the opposite direction were observed for the negative regulator SOX4 and the tumor and acinar genes (Figure A3D, F, H and J). Thus, SOX4 expression and activity positively correlates with tumor genes but negatively correlates with acinar genes while the opposite is true for RBPJL (Figure A3K and L).

PDAC-associated genes are increased during ADM of normal pancreas

We next examined the expression pattern of a selected set of 345 genes previously identified as those associated with the pancreatic acinar/ductal phenotype[30,31] or genes associated with the onset or progression of PDAC[30,32–34] (Table A2). Comparing the ADM expression data to those data obtained from published single cell RNA sequencing[31] revealed that

as expected, ductal genes were increased at day 6 while acinar genes were decreased at day 6 of ADM (Figure 5). Comparisons between the ADM data from our study and those data obtained from 4 published studies of PDAC gene expression showed that the day 6 ADM samples contained higher expression of those tumor-associated genes or genes that are increased in PDAC while the reverse was true at day 0 (Figure 5). These findings demonstrate similar trends of genes differentially expressed during in vitro ADM of normal pancreas compared to those genes that are differentially expressed in PDAC.

Our data confirm that Matrigel alone can induce ADM of normal human pancreas. To further explore the impact of additional factors on the molecular and morphological features of ADM, 5% FBS was added to the cell culture media. The percentage of cells undergoing ADM in the presence or absence of FBS was compared for 3 different donors' tissues. ADM was significantly enhanced in the presence of FBS (Figure 6A). RNA sequenced from the 3 plus FBS cultures (day 6 of ADM) was compared to the data from 14 donors minus FBS (day 6). The top 3 enriched pathways (all categories) from the IPA include TNF, AGT, and IL1B. Applying the gene set associated with KRAS addiction to the GSEA[35] showed positive enrichment in the FBS compared to the minus FBS-treated ADM cultures (Figure 6B and C). The GSEA for 2 cytokines known to induce ADM (TNF and IL17)[36] revealed that both TNF and IL17 were positively enriched when the acini were cultured with serum (Figure A5).

Discussion

We describe here a robust, in vitro 3-D model to examine human exocrine cell pancreatic plasticity with morphological and molecular features of ADM. We report that normal human pancreatic acini cultured in serum-free conditions on growth factor reduced Matrigel was sufficient to induce ADM. However, we find that acini cultured with FBS underwent more robust ADM compared to serum-free cultures and that pathways and gene sets were enriched with serum including KRAS (Figure 6). Several differences in the culture conditions exist between the present study and previously published work on human ADM in vitro models. The research from the Rooman and Houbracken laboratories transdifferentiated acinar cells in suspension cultures in media supplemented with FBS.[24–26] Zhang et al. cultured primary human pancreatic acini on Matrigel in media supplemented with 1% FBS, dexamethasone, and TGF-α.[37] Liu et al. induced in vitro ADM in normal human pancreatic acini cultured in serum-free conditions in Matrigel supplemented TGF-β.[27] Of 11 cytokines evaluated as additives, including TGF-α, only TGF-β promoted the conversion of human acinar cells to CD133+ ductal-like cells; the authors conclude that human and mouse acinar tissue require different signals to induce ADM. In our hands, adding TGF-β to the culture media had the opposite effect and reduced duct formation (Figure A1A and B). Thus, our findings more closely align with those of Baldan,[25] et al., rather than Liu,[27] et al. The culture conditions and components for the present study as well as other published studies using human ADM assays [24–27,37] are listed in Table A3.

A large number of genes were differentially expressed between day 0 and day 6 of ADM (Figure 2). Moreover, many highly significant regulons and regulon activity profiles associated with ADM were obtained (Figure 4). There appears to be a small but perhaps

significant sex difference (Figure 2B) that may be due to the inclusion of Y-chromosome–linked genes in the dataset. These data illustrate that not only are there profound differences in the expression and activity of acinar and ductal genes during ADM but also that our methodology for performing gene expression analysis is suitable for primary cells derived from pancreas that has traditionally been difficult to work with due to digestive enzyme release during exocrine cell isolation.

In a gene expression network of regulators-regulons, a phenotypic outcome is a result of cooperation and competition of multiple transcription factors and transcriptional regulators within the network. We provide correlations of dual regulons that influence shared, predicted target genes including those that effect shared target genes in the same direction (Figure A4) and those that impact shared target genes in the opposite directions (Figure A3). Some of the dual regulons described here have been experimentally verified while others have not. An example of an experientially validated dual regulon is BHLHA15~RBPJL that promoted acinar gene expression including CEL and PDE3B (Figure A4). RBPJL is part of the PTF1 transcriptional complex and together with BHLHA15 (MIST1) co-regulate many genes involved in specialized pancreatic acinar cellular processes.[38]

Caution should be exercised when comparing the results of ADM performed using acinar cells from GEMMs to those using healthy human pancreatic acinar tissue. We report that many transcriptional regulons that are activated or repressed during ADM in mice were recapitulated in human ADM. These include decreased expression and activity of acinar-associated transcriptional regulons shown to regulate ADM in GEMMs (BHLHA15,[39] GATA4,[40] PTF1A,[18] RBPJL,[41] and XBP1[42]) and an increase in ductal-associated and progenitor-associated regulons such as HNF1B,[43] SOX11,[44] SOX4,[45] and STAT2/6[46] (Figure 4D). Transcription factors previously reported as driving ADM in mice (KLF4,[47,48] ATF3,[49] and FOSL1[50]) were suppressed during ADM in our 3-D model (Figure 4D). SOX9 is a well-known progenitor cell marker whose expression is increased during in vitro human ADM.[25–27] While SOX9 mRNA increased 2-fold by qPCR (Figure 1B), we did not detect SOX9 as a significant regulon (Figure 4D). Deletion of SOX9 in the presence of oncogenic *Kras* completely blocked development of ADM and PanINs in GEMMs.[14] However, in the context of normal pancreas with wild type *KRAS*, the contribution of SOX9 in ADM may be more nuanced.

Several noteworthy differences exist between experimental in vitro models of mouse and human ADM. In vitro ADM is typically studied in very young mice (6–8 weeks of age), whereas human studies such as ours used mostly adult pancreata (Table A1). Mouse acini undergo ADM when cultured with collagen/TGF-α [13,22] or on growth factor reduced Matrigel cultured in the absence of TGF-α.[20,51] We and others[24–26] induced ADM in human tissues in the absence of additives such as TGF-α or TGF-β. Unlike its counterpart in GEMMs, all published work with human in vitro ADM has been performed on normal pancreatic acinar cells[24–27] rather than pancreatitis or PDAC-derived acini. Despite these differences, it is interesting that such a large number of PDAC-associated genes highly correlate with the gene expression/regulon activity observed in healthy pancreas undergoing ADM (Figures 5 and 6). Since many PDAC-related genes and pathways correlate with

ADM, our approach of studying ADM in normal human pancreas may be used to further advance the mechanism of human ADM and the contributions of ADM to human PDAC.

Methods

Human pancreatic acini

Fresh islet-depleted cell fractions containing digested acinar clusters from cadaveric pancreas donors were shipped overnight in PIM-T media (1% PIM-G; 2.5% AB serum; 10 μg/mL ciprofloxacin hydrochloride; 100 μg/mL Trypsin Inhibitor from Glycine Max) from pancreatic isolation centers: NIDDK Integrated Islet Distribution Program (Dr Joyce Niland, PI), University of Miami (Dr Camillo Ricordi, Director), University of Pennsylvania (Dr Ali Naji, Director), Alleghany Islet Isolation Facility (Dr Rita Bottina, Director), nPOD Islet Isolation project (Drs. Clayton Mathews and Alberto Pugliese, Directors), and Prodo Laboratories, Inc. (Aliso Viejo, CA). The study protocol was reviewed and approved as classified as “Non-Human Subjects” by the University of Florida Institutional Review Board, an independent ethics committee (IRB201902530), waiving the need for consent. Donor demographics are presented in Table A1.

3-D culture for human ADM

Upon arrival, the aqueous pancreas digest was left undisturbed for several minutes, then acinar clusters were collected from the bottom of the bottle using a serological pipette. The cells were resuspended and passed through a series of cell strainers (pluriSelect) in the following sequence: 500 μm then 300 μm then 200 μm then 100 μm. The filtrate was centrifuged at 700x g for 3 minutes at 4°C and the cell pellet was resuspended in ice cold 50:50 DMEM (4.5 g/L D-Glucose) and F12K Nutrient Mixture. The cell suspension was diluted accordingly with media (such that there will be approximately 400 acinar clusters per well of a 96-well plate) and mixed with growth-factor reduced ice cold Matrigel (Corning) at a 1:1 ratio and plated in a 96-well plate at 200 μl per well. The plate was incubated at room temperature for 10 minutes, then at 37°C for 20 minutes to solidify the Matrigel. Cell cultures were supplemented with 100 μl of warm 50:50 DMEM:F12K and 0.1 mg/mL soybean trypsin inhibitor (Sigma) and maintained at 37°C in 5% CO_2. Media were replenished daily.

Viability of cultured human acini and ductal cells

Matrigel cultures were rinsed 3 times with 400 μl warm PBS, then incubated in 100 μl of 10 μM calcein AM (Thermo Fisher) for 20–30 minutes at 37°C. Fluorescence was then imaged and photographed at 495 nm excitation using a Nikon Ts-S/L100 epifluorescence inverted microscope.

RNA isolation

Matrigel cultures were rinsed once from 96-well plates with 200 μl of cold-PBS. The Matrigel was removed from the cells from both the day 0 and day 6 cultures using low speed centrifugation at 4°C and the cells were lysed in 700 μL of Trizol reagent as previously noted.[28] Total RNA was extracted from Trizol lysate using Qiagen miRNesay Mini Kit (Qiagen, 21700r) as per the protocol’s instructions. RNA was eluted in 30 μL

RNase/DNase–free water. RNA was quantified using a NanoDrop spectrophotometer and RNA integrity was assessed using the Agilent TapeStation RNA screen. RNA samples with RINs more than 7 were used for cDNA library preparation.

qRT-PCR

Sixty ng of total RNA was converted to cDNA in a 20-μl RT reaction using random primers and Moloney murine leukemia virus reverse transcriptase (Thermo). qPCR was performed using the QuantStudio 7 Flex Real-Time PCR System (Thermo). Data are presented using the $2^{-\Delta\Delta CT}$ method relative to 18S rRNA. Primer sequences are available upon request.

Library preparation for NovaSeq6000 sequencing

RNAseq libraries were constructed using 60 ng of total RNA (each sample processed individually) as input. The preparation was performed using the reagents provided in the NEBNext Ultra II Directional RNA Library Prep Kit for Illumina (NEB #E7760S, New England Biolabs, USA), in conjunction with the NEBNext Poly(A) mRNA Magnetic Isolation Module (NEB #E7490) and the NEBNext Multiplex Oligos for Illumina (96 Unique Dual Index Primer Pairs, NEB #6440s). Briefly, RNA was fragmented in a solution containing divalent cations, with incubation at 94°C. Next, first-strand cDNA synthesis was performed using reverse transcriptase and oligo(dT) primers. Synthesis of double-stranded cDNA was done using the 2nd strand master mix provided in the kit, followed by end-repair and dA-tailing. At this point, Illumina-specific adaptors were ligated to the sample. Library enrichment and indexing were performed using UDI barcoded primers and 13 cycles of amplification, followed by purification with NEBNext Sample Purification Beads (NEB #E7767S). The library size and mass were assessed by analysis in the Agilent TapeStation using a DNA1000 Screen Tape. Typically, a narrow distribution with a peak size approximately 300 bp was observed. Quantitative PCR was used to validate the library's functionality, using the KAPA library quantification kit (Kapa Biosystems, catalog number: KK4824) and monitoring on the ABI7900HT real-time PCR system. In preparation for sequencing on the NovaSeq6000 Illumina sequencer (see below), 35 uniquely barcoded libraries were normalized to 2.5 nM and pooled (equimolarly).

Illumina NovaSeq6000 sequencing

Normalized libraries were submitted to the Free Adapter Blocking Reagent protocol (FAB, Cat# 20024145) to minimize the presence of adaptor-dimers and index hopping rates. The library pool was diluted to 0.8 nM and sequenced on one S4 flow cell lane (2 × 150 cycles) of the Illumina NovaSeq6000. The instrument's computer used the NovaSeq Control Software v1.6. Cluster and SBS consumables were v1.0. The final loading concentration of the library was 160 pM with 1% PhiX spike-in control. One lane generated 3.27 billion paired-end reads (981.5 Gb) with an average Q30% ≥ 92.5% and Cluster PF = 85.4%. FastQ files were generated using the BCL2fastQ function in the Illumina BaseSpace portal. An average of 93.4 million paired-end reads per sample after demultiplexing. Curated datasets were posted to the Gene Expression Omnibus repository under accession number GSE179248.

Transcriptional activity of genes with known functions

We annotated 6 sets of genes previously associated with acinar/ductal phenotype of pancreas or genes associated with onset or progression of PDAC, from the literature. Annotated gene sets are included known PDAC-related genes,[33] upregulated genes identified in the meta-analysis of PDAC tumors,[32] and early stage PDAC.[34] The acinar/ductal specific genes and transcription factors are adopted from[30,31,52] (Table A2 for the complete list of genes and sources).

Gene regulatory network analysis

A regulatory network of transcription factors and their target gene sets (eg, regulons) was built using the gene expression data. We then identified transcription factors that are linked to more genes in the upregulated or downregulated target gene sets than would be expected by chance. Transcription factors used in this analysis consist of a curated list of high confidence human transcription factors.[53] We inferred the relative activity of 462 candidate regulator genes by obtaining a list of regulator genes from DoRothEA which is a gene set resource containing signed transcription factor-target interactions.[53] We used the RTN method (Reconstruction of Transcriptional regulatory Networks)[54] to identify the important regulator-targets associations that controls ADM expression program. To identify transcription factors that are drivers or suppressors of ADM, we divided the regulon into 2 sets of activated and repressed genes for each significant transcription factor based on the coefficient values. The regulon activity for all TFs are estimated by 2-tailed GSEA function in RTN package.[55,56] We used Regulon activity profiles to identify the association of each regulon to pre-ADM of post-ADM phenotype.[57] RTNduals package[29] was used to identify significant co-regulatory associations between regulons (ie, dual regulons).

Gene regulatory network analysis

The known and putative gene regulatory networks were reconstructed in R using the RTN package[29] for visualization. This computational framework establishes interactions and structure of the network by mapping the interactions between upregulated transcription factors identified through motif enrichment and their respective heterogeneous genes identified by HeteroPath. GSEA (Broad Institute) and Ingenuity Pathway Analysis (Qiagen) were used as intended by the developers.

Conclusion

Our findings demonstrate that regulation of many of the transcription factors and pathways that occur in PDAC are recapitulated using this human organoid model of normal pancreatic acini and support the relevancy of human in vitro models to study pancreas cancer pathogenesis and exocrine cell plasticity.

Supplementary Material

Refer to Web version on PubMed Central for supplementary material.

Funding:

This work was supported by grants F31CA220937 (J.K.B), 3R01CA172310-08S1 (C.P.). Human pancreatic non-islet cells were provided by the NIDDK-funded Integrated Islet Distribution Program (IIDP) (RRID:SCR _014387) at City of Hope, NIH Grant # 2UC4DK098085. Research reported in this publication was supported by the National Cancer Institute, Center for Reducing Cancer Health Disparities of the National Institutes of Health under award numbers U54CA233396, U54CA233444, & U54CA233465, which support the Florida-California Cancer Research Education and Engagement (CaRE^2) Health Equity Center.

Abbreviations used in this paper

ADM	acinar ductal metaplasia
GEMM	Genetically engineered mouse model
GSEA	Gene set enrichment analysis
PanIN	pancreatic intraepithelial neoplasia
PCA	Principle component analysis
PDAC	pancreatic ductal adenocarcinoma
RIN	RNA integrity number
TF	Transcription factors

References

1. Siegel RL, Miller KD, Fuchs HE, et al. Cancer statistics, 2021. CA Cancer J Clin 2021;71:7–33. [PubMed: 33433946]
2. Rahib L, Smith BD, Aizenberg R, et al. Projecting cancer incidence and deaths to 2030: the unexpected burden of thyroid, liver, and pancreas cancers in the United States. Cancer Res 2014;74:2913–2921. [PubMed: 24840647]
3. Prasad NB, Biankin AV, Fukushima N, et al. Gene expression profiles in pancreatic intraepithelial neoplasia reflect the effects of Hedgehog signaling on pancreatic ductal epithelial cells. Cancer Res 2005;65:1619–1626. [PubMed: 15753353]
4. Collins MA, Bednar F, Zhang Y, et al. Oncogenic Kras is required for both the initiation and maintenance of pancreatic cancer in mice. J Clin Invest 2012;122:639–653. [PubMed: 22232209]
5. Grippo PJ, Sandgren EP. Acinar-to-ductal metaplasia accompanies c-myc-induced exocrine pancreatic cancer progression in transgenic rodents. Int J Cancer 2012;131:1243–1248. [PubMed: 22024988]
6. Hingorani SR, Petricoin EF, Maitra A, et al. Preinvasive and invasive ductal pancreatic cancer and its early detection in the mouse. Cancer Cell 2003;4:437–450. [PubMed: 14706336]
7. Krah NM, Narayanan SM, Yugawa DE, et al. Prevention and reversion of pancreatic tumorigenesis through a differentiation-based mechanism. Dev Cell 2019;50:744–754 e4. [PubMed: 31422917]
8. Desai BM, Oliver-Krasinski J, De Leon DD, et al. Preexisting pancreatic acinar cells contribute to acinar cell, but not islet beta cell, regeneration. J Clin Invest 2007;117:971–977. [PubMed: 17404620]
9. Grippo PJ, Nowlin PS, Demeure MJ, et al. Preinvasive pancreatic neoplasia of ductal phenotype induced by acinar cell targeting of mutant Kras in transgenic mice. Cancer Res 2003;63:2016–2019. [PubMed: 12727811]
10. Guerra C, Schuhmacher AJ, Canamero M, et al. Chronic pancreatitis is essential for induction of pancreatic ductal adenocarcinoma by K-Ras oncogenes in adult mice. Cancer Cell 2007;11:291–302. [PubMed: 17349585]

11. Habbe N, Shi G, Meguid RA, et al. Spontaneous induction of murine pancreatic intraepithelial neoplasia (mPanIN) by acinar cell targeting of oncogenic Kras in adult mice. Proc Natl Acad Sci U S A 2008;105:18913–18918. [PubMed: 19028870]
12. Johnson BL, d'Alincourt Salazar M, Mackenzie-Dyck S, et al. Desmoplasia and oncogene driven acinar-to-ductal metaplasia are concurrent events during acinar cell-derived pancreatic cancer initiation in young adult mice. PLoS One 2019;14:e0221810. [PubMed: 31490946]
13. Liou GY, Doppler H, Braun UB, et al. Protein kinase D1 drives pancreatic acinar cell reprogramming and progression to intraepithelial neoplasia. Nat Commun 2015;6:6200. [PubMed: 25698580]
14. Kopp JL, von Figura G, Mayes E, et al. Identification of Sox9-dependent acinar-to-ductal reprogramming as the principal mechanism for initiation of pancreatic ductal adenocarcinoma. Cancer Cell 2012;22:737–750. [PubMed: 23201164]
15. Strobel O, Dor Y, Alsina J, et al. In vivo lineage tracing defines the role of acinar-to-ductal transdifferentiation in inflammatory ductal metaplasia. Gastroenterology 2007;133:1999–2009. [PubMed: 18054571]
16. Bockman DE, Merlino G. Cytological changes in the pancreas of transgenic mice overexpressing transforming growth factor alpha. Gastroenterology 1992;103:1883–1892. [PubMed: 1451981]
17. Chuvin N, Vincent DF, Pommier RM, et al. Acinar-to-Ductal metaplasia induced by transforming growth factor beta facilitates KRAS(G12D)-driven pancreatic tumorigenesis. Cell Mol Gastroenterol Hepatol 2017;4:263–282. [PubMed: 28752115]
18. Krah NM, De La O JP, Swift GH, et al. The acinar differentiation determinant PTF1A inhibits initiation of pancreatic ductal adenocarcinoma. Elife 2015;4:e07125. [PubMed: 26151762]
19. Morris JPt Cano DA, Sekine S, et al. Beta-catenin blocks Kras-dependent reprogramming of acini into pancreatic cancer precursor lesions in mice. J Clin Invest 2010;120:508–520. [PubMed: 20071774]
20. da Silva L, Jiang J, Perkins C, et al. Pharmacological inhibition and reversal of pancreatic acinar ductal metaplasia. Cell Death Discov 2022;8:378. [PubMed: 36055991]
21. Backx E, Coolens K, Van den Bossche JL, et al. On the origin of pancreatic cancer. Cell Mol Gastroenterol Hepatol 2022;13:1243–1253. [PubMed: 34875393]
22. Means AL, Meszoely IM, Suzuki K, et al. Pancreatic epithelial plasticity mediated by acinar cell transdifferentiation and generation of nestin-positive intermediates. Development 2005;132:3767–3776. [PubMed: 16020518]
23. Paoli C, Carrer A. Organotypic culture of acinar cells for the study of pancreatic cancer initiation. Cancers (Basel) 2020;12:2606. [PubMed: 32932616]
24. Backx E, Wauters E, Baldan J, et al. MECOM permits pancreatic acinar cell dedifferentiation avoiding cell death under stress conditions. Cell Death Differ 2021;28:2601–2615. [PubMed: 33762742]
25. Baldan J, Houbracken I, Rooman I, et al. Adult human pancreatic acinar cells dedifferentiate into an embryonic progenitor-like state in 3D suspension culture. Sci Rep 2019;9:4040. [PubMed: 30858455]
26. Houbracken I, de Waele E, Lardon J, et al. Lineage tracing evidence for transdifferentiation of acinar to duct cells and plasticity of human pancreas. Gastroenterology 2011;141:731–741, 741.e1–4. [PubMed: 21703267]
27. Liu J, Akanuma N, Liu C, et al. TGF-beta1 promotes acinar to ductal metaplasia of human pancreatic acinar cells. Sci Rep 2016;6:30904. [PubMed: 27485764]
28. Da Silva L, Bray JK, Bulut G, et al. Method for improved integrity of RNA isolated from Matrigel cultures. MethodsX 2020;7:100966. [PubMed: 32637337]
29. Chagas VS, Groeneveld CS, Oliveira KG, et al. RTNduals: an R/Bioconductor package for analysis of co-regulation and inference of dual regulons. Bioinformatics 2019;35:5357–5358. [PubMed: 31250887]
30. Benitz S, Straub T, Mahajan UM, et al. Ring1b-dependent epigenetic remodelling is an essential prerequisite for pancreatic carcinogenesis. Gut 2019;68:2007–2018. [PubMed: 30954952]

31. Qadir MMF, Alvarez-Cubela S, Klein D, et al. Single-cell resolution analysis of the human pancreatic ductal progenitor cell niche. Proc Natl Acad Sci U S A 2020;117:10876–10887. [PubMed: 32354994]
32. Liu L, Wang S, Cen C, et al. Identification of differentially expressed genes in pancreatic ductal adenocarcinoma and normal pancreatic tissues based on microarray datasets. Mol Med Rep 2019;20:1901–1914. [PubMed: 31257501]
33. Shang M, Zhang L, Chen X, et al. Identification of hub genes and regulators associated with pancreatic ductal adenocarcinoma based on integrated gene expression profile analysis. Discov Med 2019;28:159–172. [PubMed: 31926587]
34. Wu J, Li Z, Zeng K, et al. Key genes associated with pancreatic cancer and their association with outcomes: a bioinformatics analysis. Mol Med Rep 2019;20:1343–1352. [PubMed: 31173193]
35. Singh A, Greninger P, Rhodes D, et al. A gene expression signature associated with "K-Ras addiction" reveals regulators of EMT and tumor cell survival. Cancer Cell 2009;15:489–500. [PubMed: 19477428]
36. Chiricozzi A, Guttman-Yassky E, Suarez-Farinas M, et al. Integrative responses to IL-17 and TNF-alpha in human keratinocytes account for key inflammatory pathogenic circuits in psoriasis. J Invest Dermatol 2011;131:677–687. [PubMed: 21085185]
37. Zhang H, Corredor ALG, Messina-Pacheco J, et al. REG3A/REG3B promotes acinar to ductal metaplasia through binding to EXTL3 and activating the RAS-RAF-MEK-ERK signaling pathway. Commun Biol 2021;4:688. [PubMed: 34099862]
38. Jiang M, Azevedo-Pouly AC, Deering TG, et al. MIST1 and PTF1 collaborate in feed-forward regulatory Loops that maintain the pancreatic acinar phenotype in adult mice. Mol Cell Biol 2016;36:2945–2955. [PubMed: 27644326]
39. Karki A, Humphrey SE, Steele RE, et al. Silencing Mist1 gene expression is essential for recovery from acute pancreatitis. PLoS One 2015;10:e0145724. [PubMed: 26717480]
40. Ketola I, Otonkoski T, Pulkkinen MA, et al. Transcription factor GATA-6 is expressed in the endocrine and GATA-4 in the exocrine pancreas. Mol Cell Endocrinol 2004;226:51–57. [PubMed: 15489005]
41. Masui T, Swift GH, Deering T, et al. Replacement of Rbpj with Rbpjl in the PTF1 complex controls the final maturation of pancreatic acinar cells. Gastroenterology 2010;139:270–280. [PubMed: 20398665]
42. Hess DA, Humphrey SE, Ishibashi J, et al. Extensive pancreas regeneration following acinar-specific disruption of Xbp1 in mice. Gastroenterology 2011;141:1463–1472. [PubMed: 21704586]
43. De Vas MG, Kopp JL, Heliot C, et al. Hnf1b controls pancreas morphogenesis and the generation of Ngn3+ endocrine progenitors. Development 2015;142:871–882. [PubMed: 25715395]
44. Harrison G, Hemmerich A, Guy C, et al. Overexpression of SOX11 and TFE3 in solid-Pseudopapillary Neoplasms of the pancreas. Am J Clin Pathol 2017;149:67–75. [PubMed: 29272888]
45. Huang HY, Cheng YY, Liao WC, et al. SOX4 transcriptionally regulates multiple SEMA3/plexin family members and promotes tumor growth in pancreatic cancer. PLoS One 2012;7:e48637. [PubMed: 23251334]
46. Heath H, Britton G, Kudo H, et al. Stat2 loss disrupts damage signalling and is protective in acute pancreatitis. J Pathol 2020;252:41–52. [PubMed: 32506441]
47. Brembeck FH, Rustgi AK. The tissue-dependent keratin 19 gene transcription is regulated by GKLF/KLF4 and Sp1. J Biol Chem 2000;275:28230–28239. [PubMed: 10859317]
48. Wei D, Wang L, Yan Y, et al. KLF4 is essential for induction of cellular identity change and acinar-to-ductal reprogramming during early pancreatic carcinogenesis. Cancer Cell 2016;29:324–338. [PubMed: 26977883]
49. Fazio EN, Young CC, Toma J, et al. Activating transcription factor 3 promotes loss of the acinar cell phenotype in response to cerulein-induced pancreatitis in mice. Mol Biol Cell 2017;28:2347–2359. [PubMed: 28701342]
50. Sahin F, Qiu W, Wilentz RE, et al. RPL38, FOSL1, and UPP1 are predominantly expressed in the pancreatic ductal epithelium. Pancreas 2005;30:158–167. [PubMed: 15714138]

51. Collins MA, Yan W, Sebolt-Leopold JS, et al. MAPK signaling is required for dedifferentiation of acinar cells and development of pancreatic intraepithelial neoplasia in mice. Gastroenterology 2014;146:822–834 e7. [PubMed: 24315826]

52. Hoang CQ, Hale MA, Azevedo-Pouly AC, et al. Transcriptional maintenance of pancreatic acinar identity, differentiation, and homeostasis by PTF1A. Mol Cell Biol 2016;36:3033–3047. [PubMed: 27697859]

53. Garcia-Alonso L, Holland CH, Ibrahim MM, et al. Benchmark and integration of resources for the estimation of human transcription factor activities. Genome Res 2019;29:1363–1375. [PubMed: 31340985]

54. Campbell TM, Castro MAA, de Santiago I, et al. FGFR2 risk SNPs confer breast cancer risk by augmenting oestrogen responsiveness. Carcinogenesis 2016;37:741–750. [PubMed: 27236187]

55. Castro MA, de Santiago I, Campbell TM, et al. Regulators of genetic risk of breast cancer identified by integrative network analysis. Nat Genet 2016;48:12–21. [PubMed: 26618344]

56. Robertson AG, Kim J, Al-Ahmadie H, et al. Comprehensive molecular Characterization of muscle-invasive bladder cancer. Cell 2018;174:1033. [PubMed: 30096301]

57. Corces MR, Granja JM, Shams S, et al. The chromatin accessibility landscape of primary human cancers. Science 2018;362:eaav1898. [PubMed: 30361341]

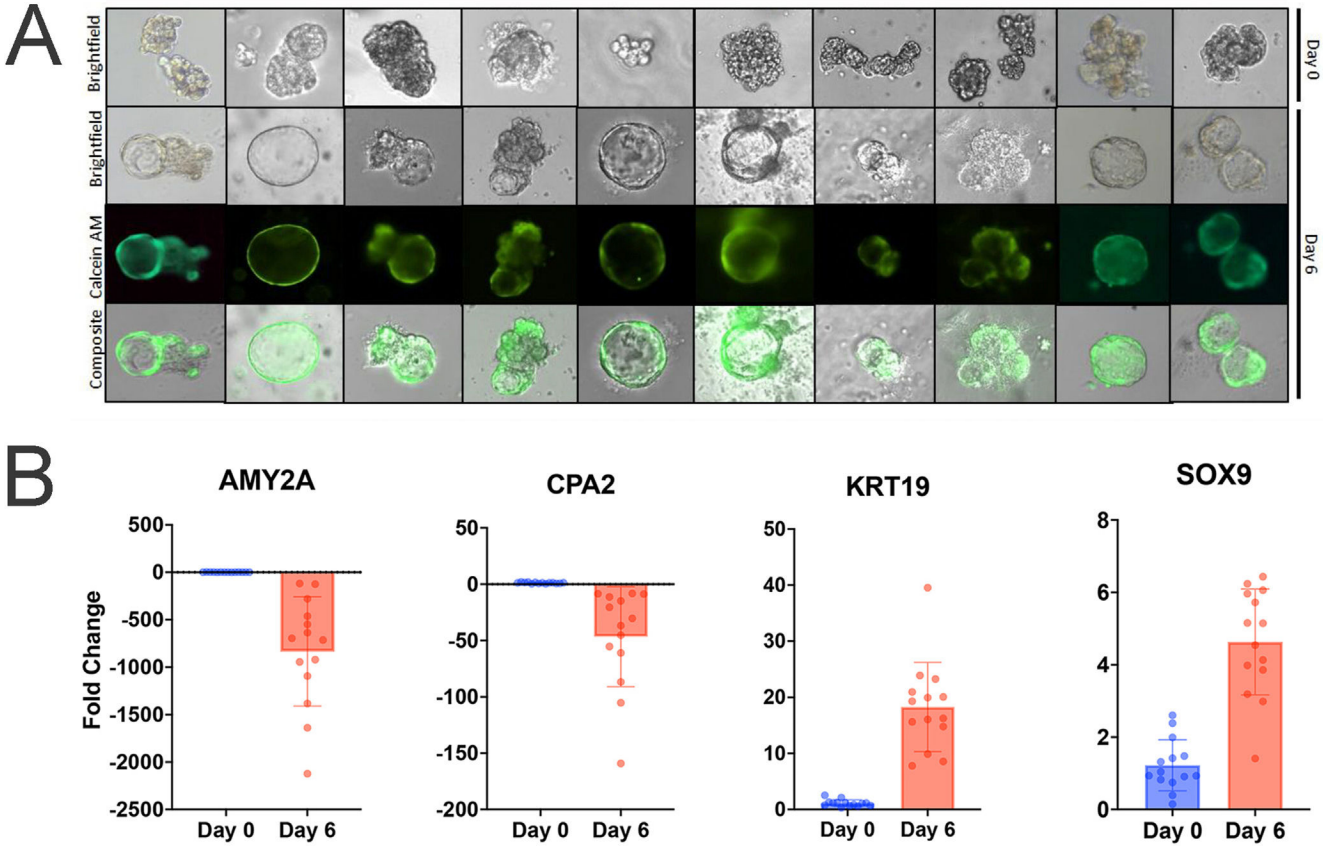

Figure 1.

Validation of human pancreatic exocrine cell ADM. (A) Representative bright field and corresponding calcein AM (green) fluorescence images of duct formation at culture day 6 from 10 pancreas donors. (B) qRT-PCR of RNA isolated at day 0 and day 6 of culture. The fold change was calculated as the gene expression at day 6 relative to day 0 normalized to 18S rRNA. Each data point represents an individual donor. Error bars std. dev. Data are presented for AMY2A, CPA1 (acinar) and KRT19, SOX9 (ductal, progenitor) genes.

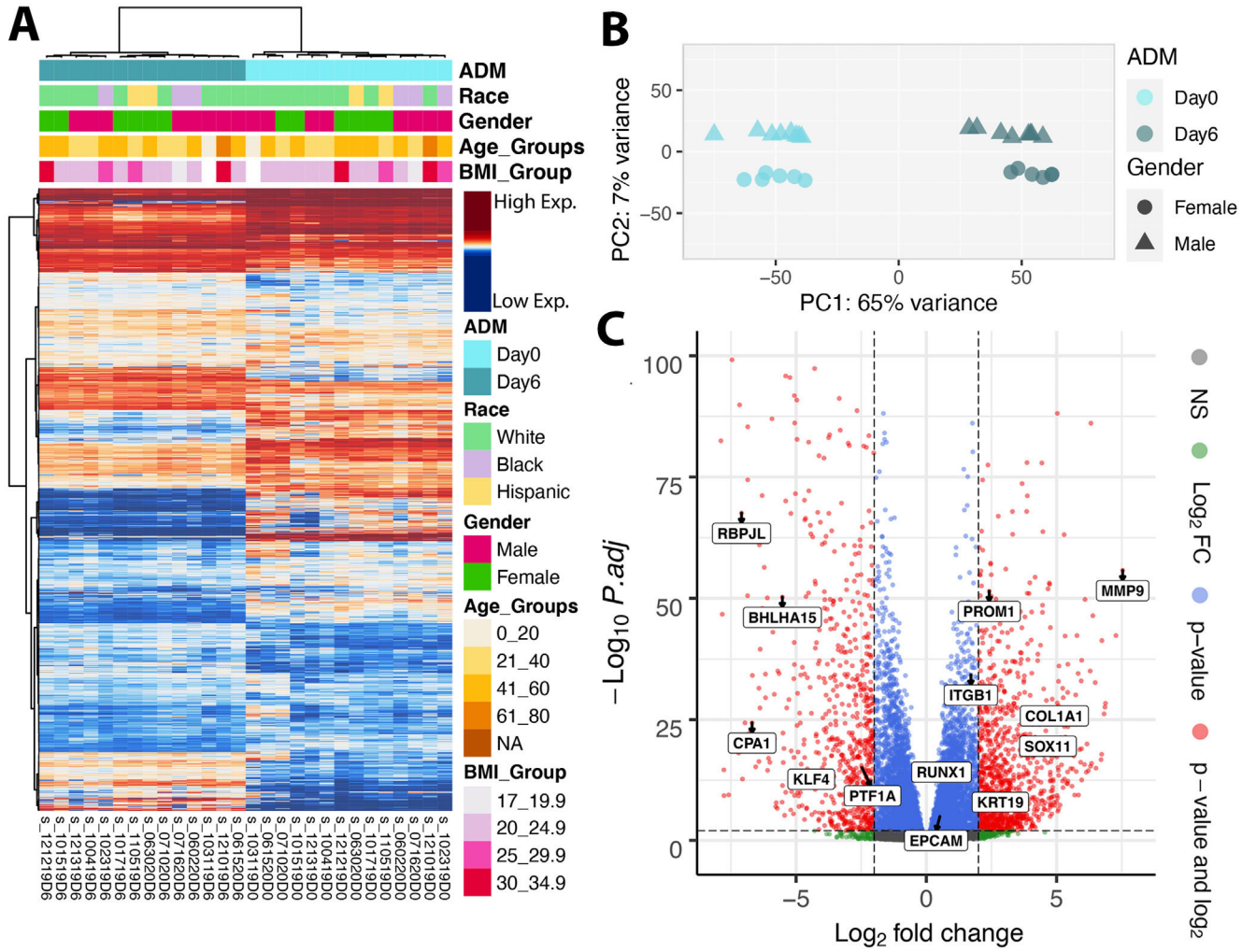

Figure 2.

Unsupervised hierarchical clustering and PCA reveal distinctive acinar cell gene expression profiles. Transcriptional profiles of primary human acinar cells were used for unsupervised hierarchical clustering (A), PCA (B) and identifying differential gene expression between day 0 and day 6 of ADM. (A) Samples were ordered by unsupervised hierarchical clustering. Heatmap columns represents 28 samples (from 14 donors). ADM status and donors' demographic data are shown at the top. Rows are the top 2000 highly expressed genes. (B) PCA of the variance in gene expression for the primary human acinar cells using all protein coding transcripts (19,626 genes). Each point represents one sample. ADM status of samples and donors' gender are specified by color and shape. (C) Volcano plot of differential gene expression of primary human acinar cells in day 0 vs day 6 of ADM. X-axis and y-axis represent log2 fold-change and statistical significance of difference between compared samples respectively. Dots represent the average values of transcripts. The significantly up-regulated and down-regulated genes are indicated with red dots. Threshold for considering a gene as significantly differentially expressed: fold change > 2 ([log2]>1; vertical dash lines (C) and adjusted *P* value of < .05 [horizontal dash line (C)].

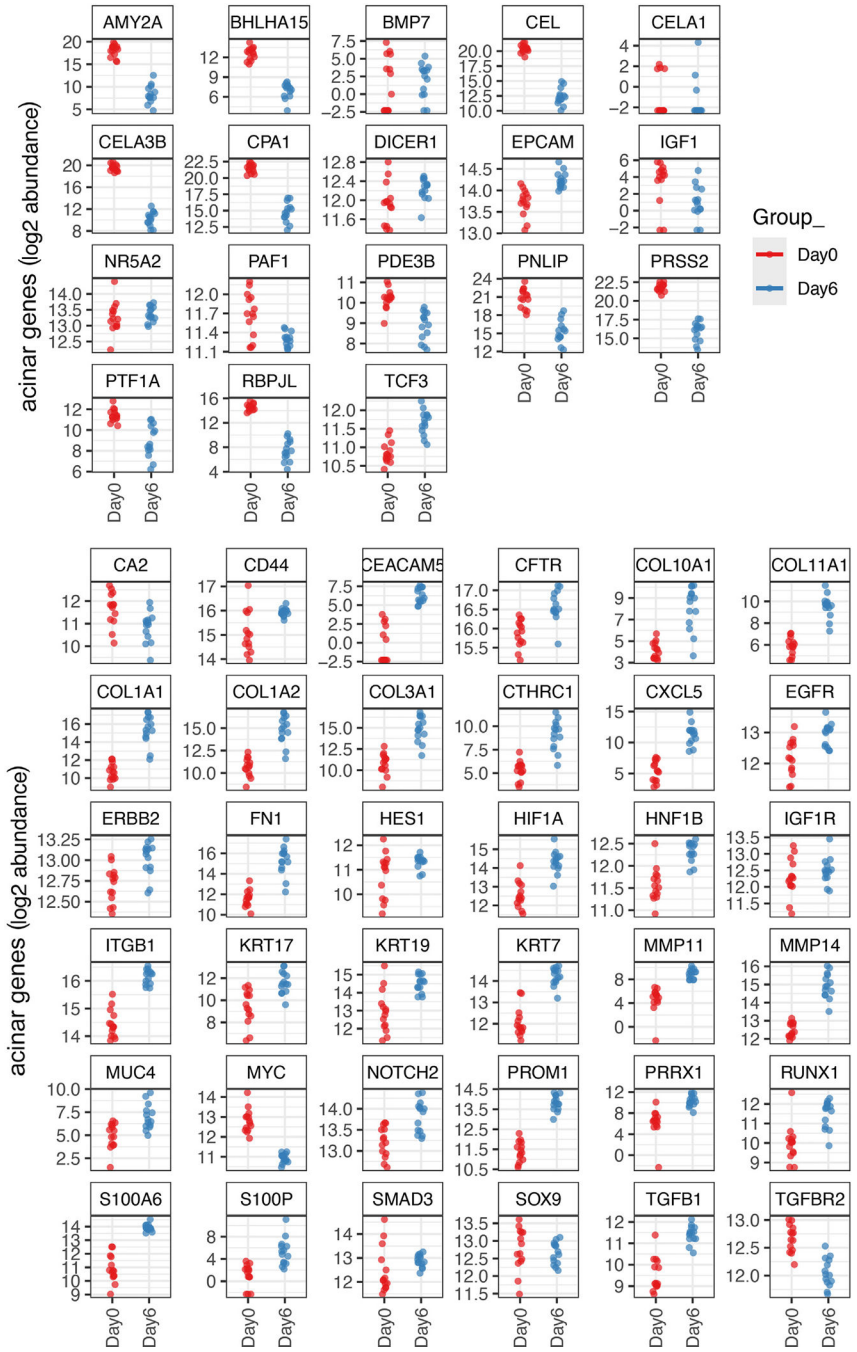

Figure 3.

Representative ADM gene expression from RNA sequencing. The expression of acinar genes (upper) or ductal/cancer genes (lower) as determined by RNA sequencing are shown at day 0 (red) and day 6 (blue). Each data point represents an individual donor.

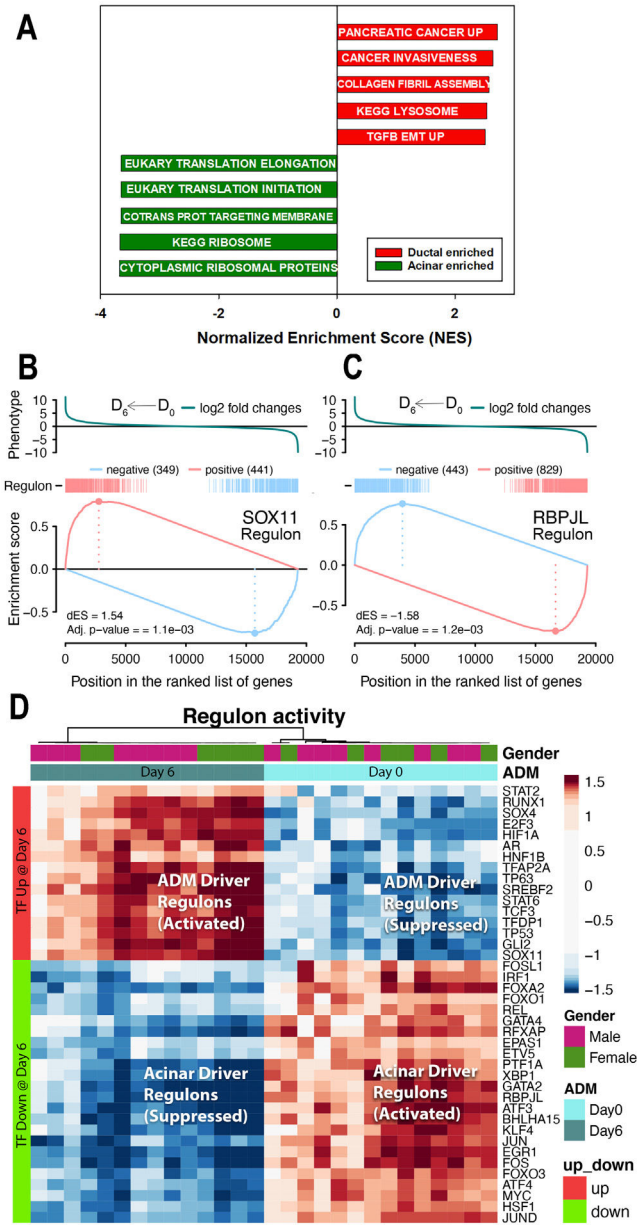

Figure 4.

GSEA and regulon activity profiles of individual samples from day 6 vs day 0 of ADM. (A) Top 5 positively enriched ductal pathways (red) and top 5 negatively enriched acinar pathways (green) on day 6 of ADM. Two-tailed GSEA graph illustrating the activity and directionality of regulons associated with the transcription factors SOX11 (B) and RBPJL (C) during ADM. (D) Regulon activity profile for the 40 most active transcription factors regulating ADM. Transcription factors are shown on the heat map rows that promote ADM (ADM driver regulons) and those that promote the acinar state (acinar driver regulons). Heat map columns represents 28 samples (from 14 different donors).

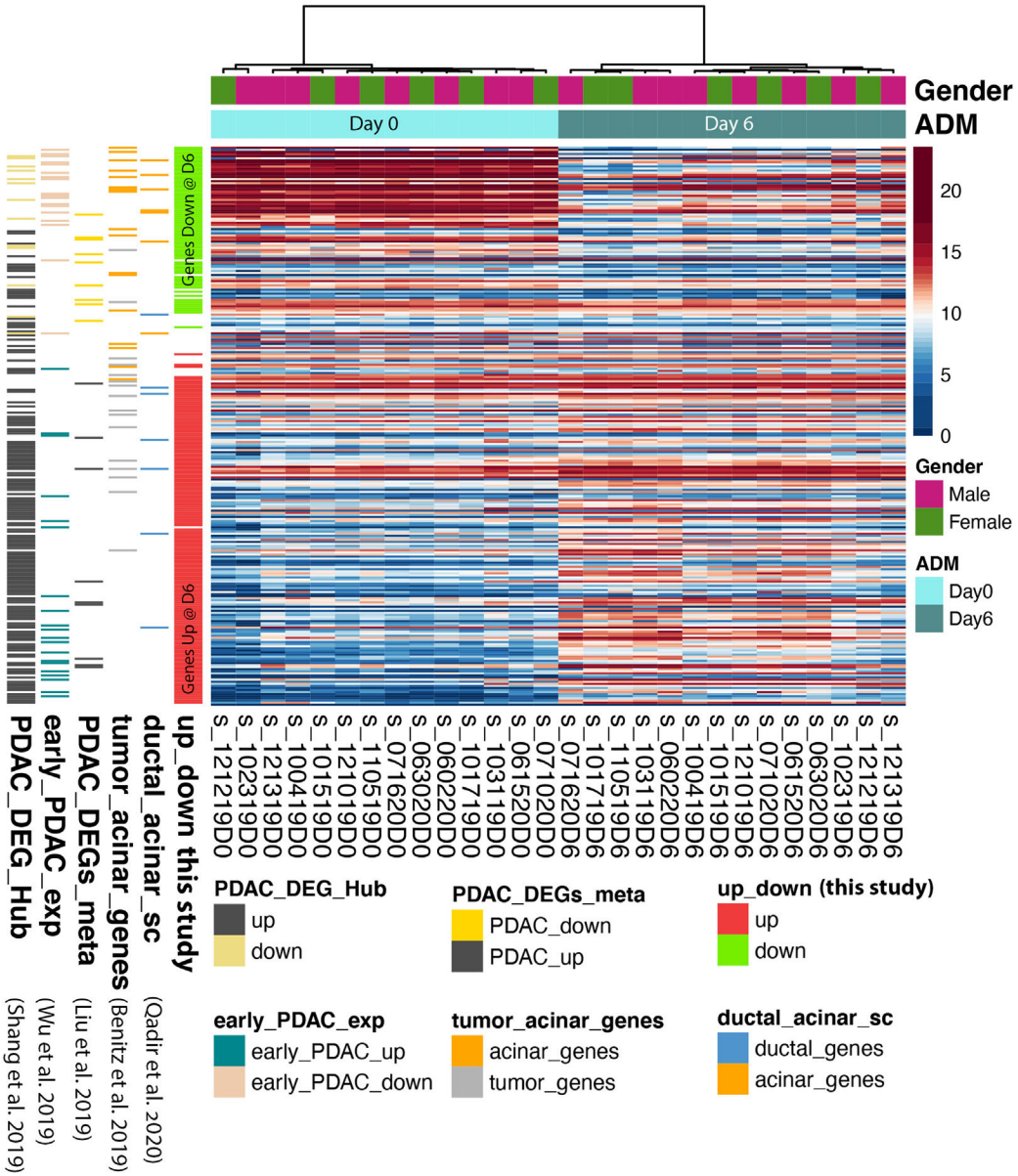

Figure 5.

Expression pattern of genes previously identified as those associated with pancreatic acinar/ductal phenotype or genes associated with onset or progression of PDAC. Three hundred sixty eight known acinar, ductal, and PDAC associated genes were selected and annotated based on the literature review. Columns are 28 samples ordered by unsupervised hierarchical clustering and rows are 268 selected genes ordered based on fold change values between day 0 and 6 of ADM. Bars indicate gene annotations based on the literature. Eighty seven percent of the selected genes (345 genes) were among the differentially expressed genes. The majority of genes upregulated on day 6 were annotated for ductal genes and transcription factors or genes overexpressed in early and later stages of PDAC tumor development.

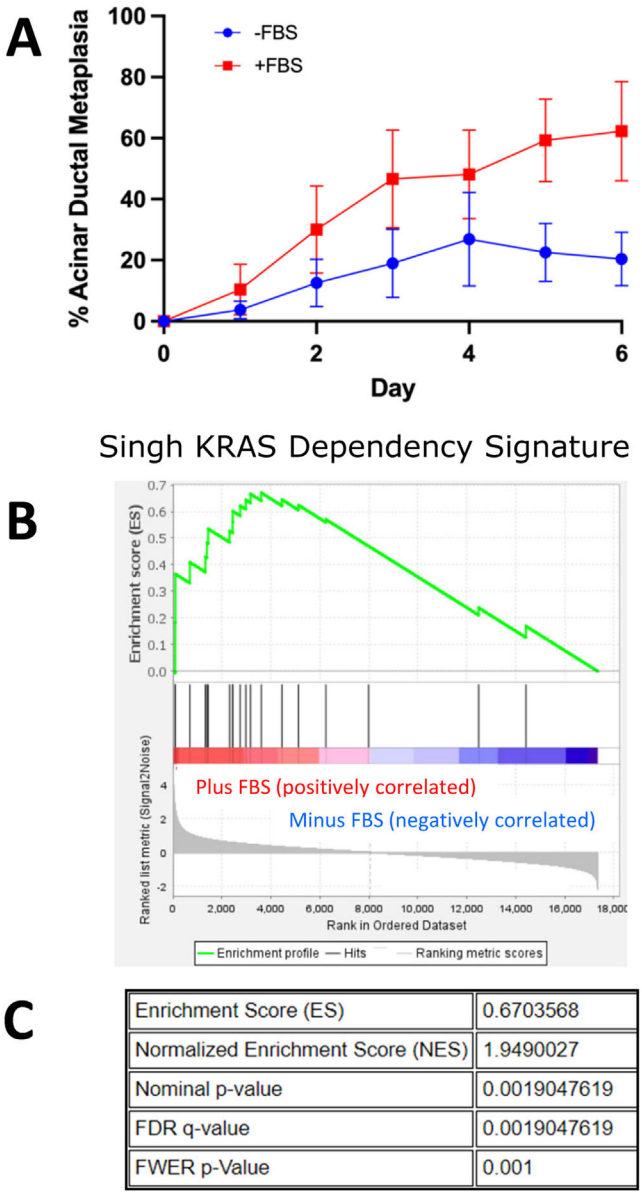

C

Enrichment Score (ES)	0.6703568
Normalized Enrichment Score (NES)	1.9490027
Nominal p-value	0.0019047619
FDR q-value	0.0019047619
FWER p-Value	0.001

Figure 6.

Serum stimulates ADM and positively enriches for KRAS gene set. The addition of 5% FBS to the cultures (A) enhanced the amount of ADM compared to those identical donor's tissues cultured in serum-free conditions. Data are the mean ± std. dev of 3 donors acinar tissues undergoing ADM over 6 days of culture. (B–C) GSEA shows positive enrichment of plus FBS (red) compared to minus FBS (blue) data for the Singh KRAS dependency signature gene set.

Table 1.

Top 10 Upstream Growth Factor Regulated Pathways Activated During ADM in Humansand Mice. There is a 30% Overlap (Bold text) Between the Top 10 Activated Growth Factor Regulated Pathways in Humans and Mice, Including the Top 2 Pathway Hits

Human ADM in vitro (present study)	−log (*P*-value)	z-score	Mouse ADM in vivo	−log (*P* value)	z-score
AGT	**32.5**	**5.54**	**Agt**	**11.5**	**9.66**
TGFB1	**46.1**	**4.1**	**Tgfb1**	**19.5**	**5.63**
GDF9	1.4	2.66	Nrg1	2.6	4.15
TGFB2	10.6	2.59	Igf1	3.8	3.62
FGF10	4.5	2.4	Hgf	4.2	3.57
INHBB	2.7	2.25	Tgfa	3.5	3.38
TGFB3	13.2	2.22	Kitlg	4.0	3.23
AREG	**6.2**	**2.11**	**Areg**	**1.7**	**3.03**
BTC	7.2	1.75	Jag1	1.6	3.01
PDGFB	4.2	1.65	Bmp6	2.1	2.42

Table 2.

Top 10 Upstream Cytokine Regulated Pathways Activated During ADM in Humans and Mice.[12] There is a 40% Overlap (Bold text) Between the Top 10 Activated Cytokine Pathways in Humans and Mice, Including the Top Pathway Hit

Human ADM in vitro (present study)	−log (*P* value)	z-score	Mouse ADM in vivo	−log (*P* value)	z-score
TNF	**43.7**	**4.02**	**Tnf**	**9.09**	**7.77**
OSM	**15.2**	**3.71**	Il1b	2.29	6.30
SPP1	3.93	3.56	CSF2	10.7	6.21
IFNL1	2.56	3.33	**Ifng**	**7.92**	**5.87**
IFNG	**32.0**	**2.55**	Wnt3a	2.68	5.06
PRL	9.91	2.40	**Il1a**	**0.58**	**4.99**
IL1A	**7.73**	**2.39**	Il33	6.04	4.52
IL19	0.51	2.00	Il6	1.75	4.06
PPBP	1.02	1.98	**Osm**	**5.95**	**3.90**
IFNL3	0.27	1.96	Il2	11.8	3.60